RSC Advances

Solution of Coupled Partial Differential Equations of a Packed Bed Reactor for SO2 Removal by Lime with Finite Element Method

Journal:	*RSC Advances*
Manuscript ID:	RA-ART-12-2014-016463.R2
Article Type:	Paper
Date Submitted by the Author:	14-Jan-2015
Complete List of Authors:	Moshiri, Hadi; Amirkabir University of Technology, Cgemical Engineering Nasernejad, Bahram; Amirkabir University of Technology (Tehran Polytechnic), Chemical Engineering Department Ale Ebrahim, Habib; Amirkabir University of Technology, Cgemical Engineering Taheri, Mahboobeh; Sarkhoon and Qeshm Gas Treating Company, R&D

Solution of Coupled Partial Differential Equations of a Packed Bed Reactor for SO_2 Removal by Lime with Finite Element Method

H. Moshiri[1], B. Nasernejad[1]*, H. Ale Ebrahim[1], and M. Taheri[2]

[1]Chemical Engineering Department, Petrochemical Center of Excellence, Amirkabir University (Tehran Polytechnic), Tehran, 15875-4413, Iran

[2]Sarkhoon and Qeshm Gas Treating Company

Abstract

Lime-based sorbents are extensively used for through-away flue gas desulphurization of coal-based power plants. In the present work, single pellet and also packed bed reactor of conventional and macro-pore lime reaction with SO_2 was simulated by applying the random pore model. The governing conservation equations for the packed bed reactor are coupled partial differential equations with three independent variables of reactor length, pellet coordinate, and time. The modeling equations were solved by a finite element solution technique. The results were well compared with some experimental conversion-time and break-through profiles from literature. Finally, effects of pore size distributions of the lime on these profiles were studied for resolving incomplete conversion problem and achieving a gypsum byproduct.

Keywords

Mathematical modeling; Packed bed reactor; Coupled partial differential equations; Finite element; SO2 removal by lime

---

*Corresponding Author, Tel./Fax: 0982164543128, Email: banana@aut.ac.ir

1 Introduction

Sulfur dioxide is one of the major air pollutant gases, which comes back to the earth by acid rains. Acid rains have harmful impressions on plants, soil, also ecology of lakes. Sources of SO_2 consist of stationary and mobile units. The most important stationary sources are pyrometallurgical units for zinc, copper, and lead roasting which produce up to 17% SO_2 in the flue gas. On the other hand, coal-based power generation units and oil and gas refineries produce lower SO_2 concentrations. Mobile sources include the automobiles which consume high-sulfur content gasoline and gas-oil (1).

To limit SO_2 emissions from automobiles, rigorous standards have been used. Gasoline and gas-oil with the ultra-low sulfur limit of 10 ppm have been produced in the refineries of the European Community since July 2010 (2). Therefore, modified catalysts for deep hydro-desulfurization of petroleum fuels have been introduced in recent works (3, 4).

One of the most important concerns of these works has been a focus on flue gas desulfurization (FGD) to minimize SO_2 emissions from stationary units. FGD methods consist of regenerative and also through-away processes (5). Regenerative FGD is suitable for high SO_2 concentrations in flue gases of copper converting and zinc sulfide roasting units. Concentrated SO_2 stream from regenerative methods can be reduced to elemental sulfur as an FGD byproduct by reducing gases such as CH_4 (6).

Through-away method is well suitable for coal-based power plants with lower SO_2 concentrations (about 1000 ppm). Lime and limestone are the most important materials as high-temperature desulfurization sorbents for throwaway FGD methods. Limestone is decomposed into CaO and CO_2 and then CaO reacts with SO_2. SO_2 reaction with lime is as follows:

$$CaO + SO_2 + ½\ O_2 = CaSO_4 \quad (1)$$

However, reaction of CaO with SO_2 shows incomplete conversion due to the pore-mouth blockage of lime particles. Because molar volume of solid product (gypsum) is about three times higher than that of lime as the solid reactant (7); therefore, this method needs a high amount of lime and also the produced $CaO/CaSO_4$ mixture cannot be used as gypsum, instead of a construction material byproduct.

SO_2 elimination by CaO is one of the most important applications of noncatalytic gas-solid reactions. Other examples of these reactions consist of reducing of metal oxides in

extractive metallurgy, roasting metal sulfide concentrates, activating carbon by steam, and regenerating of deactivated catalysts (8).

Kinetic study of gas-solid reactions is performed using a suitable mathematical model. In addition, a successful simulation model can be used to improve the efficiency of an FGD method. Various mathematical models have been introduced in the literature for estimating the conversion-time profiles of noncatalytic gas-solid reactions. Simple sharp interface model assumes a nonporous structure for the solid reactant pellet. On the other hand, volume reaction model, grain model, modified grain model, nucleation model, single pore model, and recently random pore model (RPM) have been proposed for a porous solid reactant (9).

Incomplete conversion problem due to porous solid structural changes can be predicted by some of these models, especially RPM as the most sophisticated gas-solid reaction model. Moreover, RPM considers pore size distribution of the solid reactant pellet (10-12).

Harriott et al. developed a simple model to estimate SO_2 removal in lime slurry injection into a series of coal-fired boilers (13). Lee and Koon investigated the reaction between a synthesized Ca-based sorbent and SO_2 at low temperatures and studied the effect of relative humidity, temperature, and SO_2 concentration on the break-through curves from a packed bed reactor by sharp interface model (14). Also, pore size distribution for such a sorbent was previously reported in (15).

An experimental method for solving the incomplete conversion problem in $CaO+SO_2$ reaction was proposed by Wu and co-workers (16-18). They treated the CaO sorbent by acetic acid; consequently, macro-pores were produced in the solid structure. Therefore, the pore mouth blockage problem was resolved and the complete conversion was obtained for SO_2 removal by the acid-treated CaO. However, the above mentioned study by Wu et al. was an experimental investigation. Ale Ebrahim applied RPM to the Wu et al.'s experimental conversion-time profiles for SO_2 removal by a single pellet CaO reaction (19).

Now, it is necessary to propose an appropriate mathematical model for theoretically studying the effects of pore size distribution parameters on the break-through profiles of a packed bed reactor. Therefore, a suitable function of pore size distribution curve for

resolving the incomplete conversion problem was determined in this study. Finally, the improving effect of this modified macro-pore lime on the appearance time of the break-through profile from a packed bed reactor was predicted.

In the present work, RPM was applied for $CaO+SO_2$ reaction in a single pellet and also packed bed reactor systems of conventional and macro-pore CaO-based sorbents. This modeling framework can be used for some critical calculations in terms of lime capacity predictions for SO_2 removal. The non-linear coupled partial differential equations describing either single pellet or packed bed reactor were solved by a finite element solution technique. Finite element method consists of discretization, derivation of element equations, assembly of element equations, imposition of boundary conditions, and solution of the assembled equations. The predictions were validated by some experimental conversion-time and break-through profiles from the literature. Then, effects of pore size distribution parameters of the lime sorbent on these profiles were studied. Finally, the conditions for solving incomplete conversion problem were theoretically determined. Therefore, improved lime capacity for SO_2 removal and high quality gypsum production were predicted in these conditions using the mathematical model.

2 Mathematical modeling

RPM was initially introduced by Bhatia and Perlmutter for single pellet gas-solid reaction (10-12). In the present work, this sophisticated model was applied for a packed bed reactor, and for the first time the complicated coupled partial differential equations were solved by the finite element method for the accurate simulation of SO_2 removal reaction with a packed bed of CaO.

Consider the following general reaction:

$$A(g) + \nu_B B(s) + \nu_C C(g) \rightarrow \nu_D D(s) \qquad (2)$$

Where A is SO_2, B is CaO, C is O_2, and D is $CaSO_4$.

The model assumptions are as follows:

(1) Bulk gas concentration is almost constant for a single pellet system.

(2) Pseudo-steady state approximation is valid for gas A in the pellet.

(3) The system is assumed isothermal.

(4) The pellet size is remained constant.

(5) The reaction is irreversible and first-order with respect to SO_2.

The dimensionless coupled partial differential equations of RPM for a spherical pellet geometry are as follows (10-12):

$$\frac{1}{y^2}\frac{\partial}{\partial y}\left(y^2\delta\frac{\partial a}{\partial y}\right)=\frac{\phi^2 ab\sqrt{1-\psi\ln b}}{1+\frac{\beta Z}{\psi}\left[\sqrt{1-\psi\ln b}-1\right]} \tag{3}$$

$$\frac{\partial b}{\partial \theta}=-\frac{ab\sqrt{1-\psi\ln b}}{1+\frac{\beta Z}{\psi}\left[\sqrt{1-\psi\ln b}-1\right]} \tag{4}$$

Equation (3) is reactant gas diffusion-reaction balance in the pores of a spherical pellet under pseudo- steady state approximation. Equation (4) is dimensionless solid reactant consumption rate due to reaction with gaseous reactant in RPM.

Initial and boundary conditions are as follows:

$$\theta=0 \qquad b=1 \tag{5}$$

$$y=0 \qquad \frac{\partial a}{\partial y}=0 \tag{6}$$

$$y=1 \qquad \frac{\partial a}{\partial y}=Sh*(1-a) \tag{7}$$

In Equations (3) and (4), ψ is structural parameter of RPM, which is calculated based on the initial pore size distribution of the solid reactant pellet. The relation for estimating ψ from pore size distribution function will be presented later. ϕ is Thiele modulus of RPM and proportional to the square root of rate constant ratio to the pore effective diffusivity at the beginning of the reaction, β is diffusion resistance for the solid product layer around the pores, Sh is Sherwood number for the gas-film mass transfer to the pellet surface, and Z is solid expansion or contraction factor due to the difference between molar volumes of the solid product and solid reactant as follows:

$$Z=\frac{\nu_D\rho_B M_D}{\nu_B\rho_D M_B} \tag{8}$$

When $Z<1$, the solid reactant volume is more than the product layer volume and consequently the pellet porosity increases by the progress of the reaction. For the special case of $Z=1$, the pore size remains constant during the reaction. Finally, when $Z>1$, the solid reactant volume is less than the product layer volume; thus, the pellet porosity is diminished by the reaction progress. This problem is more drastic at the pellet surface, where the gaseous reactant concentration is maximum. Therefore, the porosity at the pellet surface becomes zero (pore mouth closure) after some time in the systems with high Z values. For example, in the $CaO+SO_2$ reaction with Z=3, experimental data showed that final conversions were significantly less than unity (7). Consequently, incomplete conversion occurred, which considerably decreased the efficiency of the FGD process.

The pellet porosity at each time can be estimated as follows:

$$\left(\frac{\varepsilon}{\varepsilon_0}\right)=\left[1-\frac{(Z-1)(1-\varepsilon_0)(1-b)}{\varepsilon_0}\right] \tag{9}$$

The relation between effective pore diffusion and pellet porosity can be presented as follows (20):

$$\delta=\frac{D_e}{D_{e0}}=\left(\frac{\varepsilon}{\varepsilon_0}\right)^2=\left[1-\frac{(Z-1)(1-\varepsilon_0)(1-b)}{\varepsilon_0}\right]^2 \tag{10}$$

However, by assuming a constant tortuosity factor of the pellet during the reaction, the resulted equation (which was used in this work) is as follows:

$$\delta=\frac{D_e}{D_{e0}}=\left(\frac{\varepsilon}{\varepsilon_0}\right)=\left[1-\frac{(Z-1)(1-\varepsilon_0)(1-b)}{\varepsilon_0}\right] \tag{11}$$

Equations (10) and (11) show the variation of effective pore diffusion with the progress of the reaction due to solid structural changes (effect of Z value).

The initial effective pore diffusion coefficient of SO_2 through porous CaO pellet is estimated as follows:

$$\frac{1}{D_{e0}}=\frac{1}{\varepsilon_0}\left(\frac{1}{D_{AM}}+\frac{1}{D_{AK}}\right) \tag{12}$$

D_{AM} is molecular diffusivity of SO_2 in the gaseous mixture which is calculated by Chapman-Enskog kinetic theory and D_{AK} is Knudsen SO_2 diffusivity which is estimated

based on the average pore radius as follows (8):

$$D_{AK} = \frac{4\bar{r}}{6}\sqrt{\frac{8R_gT}{\pi M_A}} \tag{13}$$

RPM structural parameters are determined from the pore volume distribution function $v_0(r)$ by the following equations (10-12):

$$V_p = \int_0^\infty v_0(r)dr \tag{14}$$

$$\varepsilon_0 = \frac{V_p}{V_p + 1/\rho_B} \tag{15}$$

$$\bar{r} = \frac{1}{V_p}\int_0^\infty v_0(r)rdr \tag{16}$$

$$S_0 = \frac{2}{(V_p + 1/\rho_B)}\int_0^\infty \frac{v_0(r)}{r}dr \tag{17}$$

$$L_0 = \frac{1}{\pi(V_p + 1/\rho_B)}\int_0^\infty \frac{v_0(r)}{r^2}dr \tag{18}$$

$$\psi = \frac{4\pi L_0(1-\varepsilon_0)}{S_0^2} \tag{19}$$

Equation (14) is integration of pore volume distribution function to calculate the total pore volume. Then, this total pore volume can be used to compute the initial pellet porosity by equation (15). Moreover, equations (16-18) estimate the average pore radius, total pore surface area, and total pore length respectively. Finally, the RPM parameter was calculated by equation (19).

Pore volume distribution can be presented by a normal function:

$$v_0(r) = H_0 \exp[-\frac{(r-\bar{r})^2}{2\sigma_0^2}] \tag{20}$$

Finally, the conversion-time profiles of RPM for a single spherical pellet are determined using the following integral equation:

$$X(\theta) = 1 - 3\int_0^1 y^2 b(y,\theta)dy \tag{21}$$

Now, RPM must be applied to a packed bed reactor to predict the break-through curves of SO_2 from such a system with the pellets of lime sorbent. Thus, it is possible to study

the effects of operating variables on the performance of the packed bed reactor and break-through curves by RPM.

The bulk gas concentration in a packed bed reactor varies due to the reaction with solid pellets in contrast to single pellet system. Dimensionless governing equations of a packed bed reactor consisting of spherical pellets have been presented elsewhere for sharp interface and also volume reaction models (21). However, in the present work, these conservation equations were modified using RPM.

Assumptions for a packed bed reactor are as follows:

- Gas phase accumulation terms in the bed and pellet are neglected.
- Size of the pellets is remained unchanged during the reaction.
- The reaction is first order with respect to the gaseous reactant.
- The reaction is irreversible.
- The system is isothermal.

For bulk gas along the bed, the conservation equation is as follows:

$$\frac{\partial^2 w}{\partial \xi^2} - Pe\frac{\partial w}{\partial \xi} = \alpha(w - \zeta_{y=1}) \tag{22}$$

Equation (22) is dimensionless reactant bulk gas concentration balance along the reactor length and consists of convective term, dispersion, and mass transfer from bulk to the pellet surface (and subsequent reaction in the pellet pores).

The boundary conditions for the bed are expressed as:

$$\xi = 0, \quad 1 = w - \frac{1}{Pe}\frac{\partial w}{\partial \xi} \tag{23}$$

$$\xi = \Lambda, \quad \frac{\partial w}{\partial \xi} = 0 \tag{24}$$

For the gas inside the pellet, the diffusion-reaction equation is:

$$\frac{1}{y^2}\frac{\partial}{\partial y}(y^2\frac{\partial \zeta}{\partial y}) = \Phi^2 f(X)\zeta \tag{25}$$

Equation (25) is diffusion-reaction balance for gaseous reactant in the pores of the spherical pellets with suitable f(X) function from RPM (right-hand-side of equation 4, while X=1-b).

Now, *f(X)* is inserted from right-hand-side of Equation (3) for random pore model. Boundary conditions for the pellet are expressed as:

$$y = 0, \quad \frac{\partial \zeta}{\partial y} = 0 \tag{26}$$

$$y = 1, \quad \frac{\partial \zeta}{\partial y} = Bi_m (w - \zeta) \tag{27}$$

For solid reactant pellet, local conversion is:

$$\frac{\partial X}{\partial \tau} = f(X)\zeta \tag{28}$$

Equation (28) is the local (inside the pellet) solid conversion rate along the bed.

The initial condition is expressed as:

$$\tau = 0, \quad X = 0 \tag{29}$$

Dimensionless variables for packed bed are defined as follow:

$$\xi = \frac{x}{R} \tag{30a}$$

$$y = \frac{r_p}{R} \tag{30b}$$

$$\zeta = \frac{C_A}{C_{Ab0}} \tag{30c}$$

$$w = \frac{C_{Ab}}{C_{Ab0}} \tag{30d}$$

$$\tau = \nu_B \frac{k_s C_{Ab0} t}{C_{B0}} \tag{30e}$$

$$\Lambda = \frac{L}{R} \tag{30f}$$

Dimensionless parameters for packed bed are expressed as follow:

$$Pe = \frac{uR}{D_L} \tag{31a}$$

$$\alpha = \frac{1-\varepsilon}{\varepsilon} \frac{3k_m R}{D_L} \tag{31b}$$

$$\Phi^2 = \frac{\nu_A k_s R^2}{D_e} \tag{31c}$$

$$Bi_m = \frac{k_m R}{D_e} \tag{31d}$$

3 Finite element solution method

In this work, non-linear coupled partial differential equations of random pore model were solved by finite element method. Detailed description of this solution technique has been presented in the previous works for the single pellet system (22, 23). However, for a packed bed reactor, finite element method was applied for the first time in the present work.

Weak form development and finite element solution technique are described in this section. Steps involved in finite element analysis of the problem are as follows:

1- Discretization of the given domain in a collection of preselected finite elements: For a spherical pellet, the equations are functions of only the radial coordinate r because of its symmetrical geometry. Consequently, finite elements for pellet may be considered only in the radial direction. Since column equation is only a function of z; then, the given domain may be discretized only in z direction.

2- Derivation of element equations for all typical elements in the mesh as:

$$[K^e]\{u^e\} = \{F^e\} \tag{32}$$

Equation (32) is applicable for either pellet or column equations. For pellet, u^e may be replaced with y_p^e and, for column, may be replaced with y_c^e.

In this work, quadratic elements either for pellet equations or column equations were selected. Then, Rayleigh Ritz method was applied which took Lagrangian interpolation functions for defining weight functions as:

$$\Psi_1 = \frac{(x - x_2)(x - x_3)}{(x_2 - x_1)(x_3 - x_1)} \tag{33}$$

$$\Psi_2 = \frac{(x - x_1)(x - x_3)}{(x_2 - x_1)(x_2 - x_3)} \tag{34}$$

$$\Psi_3 = \frac{(x - x_1)(x - x_2)}{(x_3 - x_1)(x_3 - x_2)} \tag{35}$$

For pellet equations, variable x is replaced with r and, for column equations, variable x is replaced with z. Since quadratic interpolation functions were employed for each finite element in this work, each finite element had three unknown nodal points.

3- Assembly of element equations of the whole domain;

4- Imposition of the boundary conditions of the problem;

5- Solution of the assembled equations;

6- Post-processing of the results.

Now, development of finite element equations for both single pellet and packed bed systems is discussed.

3.1 Gas profile equation inside the pellet for single pellet and also packed bed systems

Weak form equation for a typical element and spherical pellet is as:

$$I = \int_{r_a}^{r_b} W_p [\frac{1}{r^2}\frac{\partial}{\partial r}(\delta r^2 \frac{\partial y_p}{\partial r}) - \lambda y_p] r^2 dr = 0 \tag{36}$$

in which:

$$\lambda = \frac{\phi^2 b\sqrt{1-\psi \ln b}}{1+\frac{\Omega Z}{\psi}(\sqrt{1-\psi \ln b}-1)} \tag{37}$$

(r_a, r_b) is domain of the element along the radial direction. Integration by parts is used in the first term in the bracket of Equation (36) to equally distribute the spatial derivative between weight function w_p and dependent variable y_p.

$$\int_{r_a}^{r_b} [-r^2\delta \frac{\partial W_p}{\partial r}\frac{\partial y_p}{\partial r} - W_p \lambda r^2 y_p] dr = -W_p(r_b)Q_2^e - W_p(r_a)Q_1^e \tag{38}$$

in which:

$$Q_1^e = -(r^2\delta \frac{\partial a}{\partial r})_{r_a} \tag{39}$$

$$Q_2^e = (r^2\delta \frac{\partial a}{\partial r})_{r_b} \tag{40}$$

Bulk gas concentration in each element is defined as follows:

$$y_p = \sum_{j=1}^{3} y_{pj}^e \Psi_j \tag{41}$$

Matrix equations for one single element are as:

$$ke' = \int_0^{re} [-r^2 \delta \frac{\partial W_p}{\partial r} \frac{\partial y_p}{\partial r} - W_p \lambda r^2 y_p] dr \quad (42)$$

$$fe' = \{0\} \quad (43)$$

The final solution can be obtained after solving the following assembled equation by applying boundary conditions:

$$[K'] \{y_p\} = \{Q'\} \quad (44)$$

Application of boundary condition (6) results in:

$$Q(1) = 0 \quad (45)$$

Application of boundary condition (7) results in the following expressions for a single pellet system:

$$Q_{end} = Q_{end} - Sh \quad (46)$$

$$K_{end} = K_{end} - Sh \quad (47)$$

Finally, application of boundary condition (27) results in the following expressions for the packed bed system:

$$Q_{end} = Q_{end} - Bi \times y_c \quad (48)$$

$$K_{end} = K_{end} - Bi \quad (49)$$

3.2 Gas profile equation through the column in packed bed system

Multiplying of weight function by the column equation yields:

$$I = \int_{z_a}^{z_b} [W_c \frac{\partial^2 y_c}{\partial z^2} - W_c Pe \frac{\partial y_c}{\partial z} - W_c \beta (y_c - y_{patr=1})] dz \quad (50)$$

(z_a, z_b) is domain of the element along z direction in the bed. Integration by parts is used in the first term in the bracket of Equation (50) to equally distribute the spatial derivative between weight function W_c and dependent variable y_c:

$$I = \int_{z_a}^{z_b} [-\frac{\partial W_c}{\partial z} \frac{\partial y_c}{\partial z} - W_c Pe \frac{\partial y_c}{\partial z} - \beta W_c y_c] dz = \int_{z_a}^{z_b} [-\beta W_c (y_{patr=1})] dz - W_c(\Lambda) Q_2^e - W_c(0) Q_1^e \quad (51)$$

in which:

$$Q_2^e = (\frac{\partial y_c}{\partial z})_{z=z_b} \quad (52)$$

$$Q_1^e = -(\frac{\partial y_c}{\partial z})_{z=z_a} \quad (53)$$

Bulk gas concentration of column in each finite element is defined as follows:

$$y_c = \sum_{j=1}^{3} y_{cj}^e \Psi_j \quad (54)$$

The answer is obtained after solving the following equation by applying boundary conditions:

$$[K]\{y_c\} = \{Q\} + \{F\} \quad (55)$$

Matrix equations for one single element are as follows:

$$ke = \int_0^{ze} [-\frac{\partial W_c}{\partial z}\frac{\partial y_c}{\partial z} - W_c Pe \frac{\partial y_c}{\partial z} - \beta W_c y_c]dz \quad (56)$$

$$fe = \int_0^{ze} [-\beta W_c (y_{patr=1})]dz \quad (57)$$

$$fe = -\frac{\beta h_e}{6}(y_{patr=1})[141] \quad (58)$$

Application of boundary condition (23) results in:

$$Q(1) = Q(1) - Pe \quad (59)$$

$$K(1,1) = K(1,1) - Pe \quad (60)$$

Application of boundary condition (24) yields:

$$Q_{end} = 0 \quad (61)$$

3.3 Solid phase equation along the bed

Solid phase equation is solved by Runge-Kutta-Fehlberg method. The overall solid conversion along the bed may be calculated using:

$$X(t) = 1 - 3\int_0^1 r^2 b dr \quad (62)$$

4 Solution procedure for single pellet system

Solution procedure of equations for the single pellet system is as follows:

1- Solving equation (44) for the single pellet;

2- Calculating solid concentration along the bed using equation (4) for the next time step;

3- Calculating average solid conversion in the pellet using equation (62);

4- Going to the next time step and repeating the solution from step 1 until reaching the final time.

5 Solution procedure for packed bed system

Solution procedure of equations for packed bed system is as follows:

1- Discrete length of the bed uniformly from the bottom to top and also spherical pellets uniformly from the center to surface; dividing reaction time uniformly from initial to the final values;

2- Initially, guessing some values for $y_{patr=1}$ along the bed;

3- Obtaining gas profile along the bed by solving equation (54);

4- Solving equation (44) for pellets along the bed; the pellet equation must be solved for each node in z direction. After this solution, a new gas profile for $y_{patr=1}$ is obtained;

5- If the difference between initial guesses and obtained values of $y_{patr=1}$ is in the acceptable tolerance, go to Step 6; else, return to Step 1;

6- Calculating solid concentration along the bed using equation (28) for the next time step;

7- Calculating solid conversion profile along the bed using equation (62);

8- Going to next time step and repeating the solution from Step 3 until obtaining the final time step.

The preferences of finite element method with respect to conventional finite difference approach are as follows:

1- Higher accuracy with the same number of nodes.

2- Having the profile of target function between nodes.

3- Simple geometric flexibility and easier implementing of various boundary conditions.

4- Capability of solving equations in various reaction regimes, even at high Thiele modulus (diffusion control) and steep concentration profiles.

5- Solving equations in the presence of severe structural changes such as pore-mouth blockage and incomplete conversion.

6- Finally, the computational time in this work for finite element method is only a little more than finite difference technique (see section 6.1).

6 Results and discussion

6.1 Model validation

First of all, the conversion-time profiles from finite element method for a single pellet system ($CaO+SO_2$ reaction) are presented in Figure 1 and compared with the previous orthogonal collocation solution results (19) and also the experimental data from the literature (18). Structural properties of three types of limes (18) and random pore model parameters for the simulation are presented in Table 1.

Then, the break-through curves for a packed bed reactor are expressed in Figures 2 and 3 for the volume reaction model and compared with the results of finite difference solution method (21). Effect of Peclet number (axial dispersion) is presented in Figure 2, while Figure 3 shows the effect of reaction Thiele modulus. As demonstrated in Figures 2 and 3, good agreement was found between results of this work and finite difference solution (21). The computational times of equations in Figure 2 for finite element and finite difference methods are 26 sec and 22 sec respectively.

For random pore model in packed bed reactor, a comparison was made between predicted break-through curves and the experimental data in the literature (14), as given in Figure 4. It can be observed in this figure that the simulation results of this work based on random pore model for a packed bed system successfully predicted the experimental break-through data. Structural properties of sorbent (14) and its random pore model parameters are presented in Tables 2 and 3, respectively.

Therefore, accuracy of this new finite element solution technique was verified for both single pellet and packed bed systems.

6.2 Resolving incomplete conversion problem

Now, it is necessary to propose a suitable pore size distribution function for resolving incomplete conversion problem. A normal pore volume distribution function with average radius rbar, height H, and standard deviation sigma is applied in this section.

Operating conditions of (14) are selected for this purpose.

Effects of variations of normal pore size distribution on conversion-time profile are presented in Figure 5, in which a bi-modal pore size distribution (with some macro-pores) was used to simply resolve incomplete conversion problem, while, sorbent of (14) work showed incomplete conversion at very low values (5%). The pore size distribution curves are presented in Figure 6.

The same effects on the break-through curve are indicated in Figure 7, which shows that a time lag on the SO_2 break-through curve appeared for the lime with higher conversion-time profile (with macro-pores). Thus, by resolving the incomplete conversion problem, life time of a packed bed system was also considerably improved.

6.3 Producing high quality gypsum in the packed bed

Average overall solid conversion in the packed bed was calculated as about only 27% at SO_2 break-through time in Figure 7 (about 20 min). Since this value showed significant unreacted CaO in $CaSO_4$ at this time, quality of this mixture as constructive gypsum was not appropriate.

Therefore, a combination of two consecutive packed beds was proposed. Dimensionless SO_2 concentrations in two beds are indicated in Figure 8. In such a system, the average overall solid conversion in the first bed can be considerably increased. This claim is presented in Figure 9 for a combined system, which represented about 97% average overall solid conversion in the first bed after about 100 min (before the appearance of SO_2 break-through curve from the second bed). In other words, completion of overall solid conversion in the first bed was at about 80 min after the SO_2 break-through time of the first bed. However, at this final time, outlet SO_2 concentration from the second bed was negligible. Therefore, it was possible to produce high quality gypsum from the first bed in the proposed combined system.

The proposed two bed system for SO_2 removal by lime is presented in Figure 10. Valve on/off positions for this configuration is also given in Table 4.

Consequently, this construction material byproduct (gypsum) can decrease the total cost of flue gas desulfurization process by lime. Also, disposal problem of the throwaway lime-based flue gas desulfurization can be eliminated.

For preliminary reactor design of fixed bed flue gas desulfurization, the reactor volume can be evaluated based on flue gas flow-rate and a reasonable life-time of the bed. The life-time is estimated based on the present work equations and before the appearance of breakthrough curve. Indeed, fixed bed flue gas desulfurization by CaO is similar to natural gas desulfurization in petrochemical plants by small twin ZnO fixed beds. However, H_2S concentration in sweet natural gas feed is only 4 ppm with offloading-time in order of six months for each bed, while the SO_2 concentration in flue gas of a power plant is 250 times greater. Consequently for an offloading-time in order of a week, the volume of each flue gas desulfurization reactor can be ten times greater.

7 Conclusions

In this work, random pore model was applied to flue gas desulfurization by lime. The coupled partial differential conservation equations in a packed bed reactor were solved by finite element method, which provided the accurate prediction of conversion-time profiles in the literature. Moreover, random pore model coupled with the packed bed reactor equations was capable of predicting the sorbent performance as break-through curves. This modeling framework was used for proposing theoretical methods for resolving incomplete conversion problem, increasing life time of a packed bed reactor, and preparing high quality gypsum byproduct in the flue gas desulfurization by lime.

Acknowledgement

Authors acknowledge the financial support of Sarkhoon and Qeshm Gas Treating Company.

Nomenclature

$a = C_A/C_{Ab}$ = dimensionless gaseous reactant concentration

$b = C_B/C_{B0}$ = dimensionless solid reactant concentration

C_A =gaseous reactant concentration in the pellet (kmol/m^3)

C_{Ab}= bulk concentration of gaseous reactant (kmol/m^3)

C_B=solid reactant concentration (kmol/m^3)

C_{B0} =ρ_B/M_B =initial solid reactant concentration (kmol/m^3)

D_e=effective diffusivity of gas A in the pellet (m^2/s)

D_{e0}= initial effective diffusivity of gas A in the pellet (m^2/s)

D_p=effective diffusivity of gas A in the product layer (m^2/s)

D_L = dispersion coefficient in bed (m^2/s)

k=volume rate constant (1/s)

k_m= external mass-transfer coefficient (m/s)

k_s= surface rate constant (m/s)

L =total length of bed (m)

L_0= pore length per unit volume (1/m^2)

M_B=molecular weight of solid reactant (kg/kmol)

M_D=molecular weight of solid product (kg/kmol)

r =pore radius (m)

r_p = distance from the center of the pellet (m)

$\bar{r}$ = average pore radius of the pellet (m)

R =radius of the pellet (m)

S_0= reaction surface area per unit volume (1/m)

$Sh= k_m R/D_{e0}$ = Sherwood number for external mass transfer

t =time (s)

v_0(r) = pore volume distribution function (m^2/kg)

V_p =total pore volume (m^3/kg)

x = axial distance from beginning of bed (m)

$X(\theta)$ =solid conversion at each time

y =r_p/R =dimensionless position in the pellet

Z =ratio of molar volume of solid product to solid reactant

$\beta= 2k_s(1 - \varepsilon_0)/(\nu_B D_p S_0)$ = product layer resistance

ε= pellet porosity

ε_0= initial pellet porosity

$\delta= D_e/D_{e0}$= variation ratio of the pore diffusion

$\theta= k_s S_0 C_{Ab} t/[C_{B0}(1 - \varepsilon_0)] = t/\tau$= dimensionless time

ν_B= stoichiometric coefficient of the solid reactant

ν_D= stoichiometric coefficient of the solid product

ρ_B=true density of the solid reactant (kg/m^3)

ρ_D = true density of the solid product (kg/m^3)

$\varphi= R(k_s S_0/\nu_B D_{e0})^{1/2}$ = Thiele modulus for the pellet

ψ= random pore model parameter

References

1. Kirk-Othmer. Encyclopedia of Chemical Technology. New York: John Wiley and Sons; 1991.
2. Stanislaus A, Marafi A, Rana MS. Recent advances in the science and technology of ultra low sulfur diesel (ULSD) production. Catal Today. 2010;153:1-68.
3. Yin H, Zhou T, Liu Y, Chai Y, Liu C. NiMo/Al2O3 catalyst containing nano-sized zeolite Y for deep hydrodesulfurization and hydrodenitrogenation of diesel. J Natural Gas Chem. 2010;20:441-8.
4. Chen TM, Wang CM, Wang I, Tsai TC. Promoter effect of vanadia on Co/Mo/Al2O3 catalyst for deep hydrodesulfurization via the hydrogenation reaction pathway. J Catal. 2010;272:28-36.
5. Kirk-Othmer. Encyclopedia of Chemical Technology. New York: John Wiley and Sons; 1995.
6. Zhu T, Dreher A, Stephanopoulos MF. Direct Reduction of SO2 to Elemental Sulfur by Methane Over Ceria-Based Catalysts. Appl Catal B Envir. 1999;21:103-20.
7. Georgakis C, Chang CW, Szekely J. A Changing Grain Size Model for Gas-Solid Reactions. Chem Eng Sci. 1977;34:1072-5.
8. Szekely J, Evans JW, Sohn HY. Gas-Soild Reactions. New York: Academic Press; 1976.
9. Ramachandran PA, K. DL. Modeling of Noncatalytic Gas-Solid Reactions. AIChE. 1982;28:881-900.
10. Bhatia SK, Perlimutter DD. The Effect of Pore Structure on Fluid-Solid Reactions: Application to the SO2-Lime Reaction. AIChE. 1981;27:226-34.
11. Bhatia SK, Perlimutter DD. A Random Pore Model for Fluid-Solid Reactions: I. Isothermal, Kinetic Control. AIChE. 1980;26:379-86.
12. Bhatia SK, Perlimutter DD. A Random Pore Model for Fluid-Solid Reactions: II. Diffusion and Transport Effects. AIChE. 1981;27:247-54.
13. Harriott P, Ruether J, Sudhoff F. Prediction of SO2 Removal for Power Plants Using Duct Injection of Lime Slurry. American Chemical Society. 1991;5(2):254-8.
14. Lee KT, Koon OW. Modified shrinking unreacted-core model for the reaction between sulfur dioxide and coal fly ash/CaO/CaSO4 sorbent. Chemical Engineering Journal. 2009;146(1):57-62.
15. Lee KT, Mohamed AR, Bhatia S, Chu KH. Removal of sulfur dioxide by fly ash/CaO/CaSO4 sorbents. Chemical Engineering Journal 2005;114:171-7.
16. Wu S, Azhar Uddin M, Sasaoka E. Effect of Pore Size Distribution of Calcium Oxide High-Temperature Desulfurization Sorbent on Its Sulfurization and Consecutive Oxidative Decomposition. Energy & Fuels. 2005;19:864-8.
17. Wu S, Azhar Uddin M, Su C, Nagamine S, Sasaoka E. Effect of Pore Size Distribution of Lime on the Reactivity for the Removal of SO2 in the Presence of High Concentration CO2 at High Temperature. Ind Eng Chem Res. 2002;41:5455-8.
18. Wu S, Naomi S, Caili S, Sasaoka E, Azhar Uddin M. Preparation of Macroporous Lime from Natural Lime by Swelling Method with Water and Acetic Acid Mixture for Removal of Sulfur Dioxide at High-Temperature. Ind Eng Chem Res. 2002;41:1352-6.
19. Ale Ebrahim H. Application of Random-Pore Model to SO2 Capture by Lime. Ind Eng Chem Res. 2010;49:117-22.
20. Wakao N, Smith JM. Diffusion in Catalyst Pellets. Chem Eng Sci. 1962;17(11).

21. Fernandez N, Gavalas GR. Solution of Equations Describing Fluid-Solid Reaction in Packed Columns. AIChE. 1995;41:2549-55.
22. Afshar Ebrahimi A, Ale Ebrahim H, Hatam M, Jamshidi E. Finite Element Solution for Gas-Solid Reactions: Application to the Moving Boundary Problems. Chem Eng. 2008;144:110-8.
23. Afshar Ebrahimi A, Ale Ebrahim H, Hatam M, Jamshidi E. Finite Element Solution of the Fluid-Solid Reaction Equations with Structural Changes. Chem Eng. 2009;148:533-8.

Figure Captions

Figure 1) Comparison of results for finite element solution of RPM for single pellet system for various references. (line): RPM by finite element in this work, (dashed): RPM by orthogonal collocation (19), (points): literature experimental data (18)

Figure 2) Effect of axial dispersion on breakthrough curve for a packed bed reactor in volume reaction model and $\phi^2 = 100,\ \mathrm{Bi} = 50,\ \Lambda = 300,$ left: $\mathrm{Pe} = 1.1, \alpha = 3.3,$ middle: $\mathrm{Pe} = 0.11, \alpha = 0.33,$ right: $\mathrm{Pe} = 0.011, \alpha = 0.033,$ (line): finite element method in this work, (doted): finite difference results (21)

Figure 3) Effect of reaction rate constant on the shape of breakthrough curve for a packed bed reactor in volume reaction model and $\mathrm{Bi} = 50, \mathrm{Pe} = 1.1, \alpha = 3.3, \Lambda = 300,$ left: $\phi^2 = 1,$ middle: $\phi^2 = 100,$ right: $\phi^2 = 1000,$ (line): finite element method in this work, (doted): finite difference results (21)

Figure 4) Experimental and simulated desulfurization break-through curves for various SO_2 initial concentrations, reaction temperature=70^{o}C, relative humidity=60%, NO initial concentration=500 ppm. (line): RPM with finite element solution in this work, (dashed): finite difference solution for shrinking unreacted core model (14), and (points): literature experimental data (14)

Figure 5) Effect of variation of normal pore size distribution (PSD) on conversion-time profile in a single pellet, (line): after PSD correction, (dashed): before PSD correction

Figure 6) PSD curves, left: PSD before correction (14), right: PSD after correction

Figure 7) Effect of variation of normal pore size distribution on break-through curve and solid conversion for packed bed, (line): after PSD correction, (dashed): before PSD correction

Figure 8) Dimensionless SO_2 concentration through the beds in a system of two consecutive beds

Figure 9) Average overall solid conversion (left), and break-through curve (right) in a system of two consecutive beds, (line): first reactor, (dashed): second reactor

Figure 10) Two packed beds operation sequence

Tables

Table 1) Structural properties and RPM parameters for the three types of lime in figure 1

	Raw	Water Treated	Acetic Acid-Water Treated
ϕ	15.17	7.29	1.79
β	0.83	0.795	0.63
ε_0	0.56	0.72	0.86
$D_{e0}(cm^2/min)$	2.12	6.1	64
$\tau\ (min)$	32.4	30.9	24.5
ψ	0.62	0.52	2.27

Table 2) Structural properties for the coal fly ash/CaO/$CaSO_4$ sorbent

	Coal fly ash/CaO/$CaSO_4$ sorbent
$\bar{r} \times 10^5(cm)$	0.5
$V_p\ (cm^3/g)$	0.1082
ε_0	0.2412
$S_0 \times 10^{-5}(1/cm)$	1.6728
$L_0 \times 10^{-10}(1/cm^2)$	1.8940
ψ	6.4538
$D_{e0}(cm^2/min)$	0.0502

Table 3) Random pore model parameters for coal fly ash/CaO/$CaSO_4$ sorbent

SO_2 Concentration	Pe	Bi	ϕ	Ω	α	$\tau\ (min)$
1500 ppm	0.56	483	15.2	24.8	1.71	22.5
2000 ppm	0.56	483	16.5	29.1	1.71	35.3

Table 4) Valves on/off positions for two packed bed systems of figure 10 (O: Open, C: Close)

Operation Sequence	VLV-100	VLV-101	VLV-102	VLV-103	VLV-104	VLV-105	VLV-106	VLV-107	VLV-108	VLV-109	VLV-110
Col-100 A & Col-100 B	O	O	C	C	O	O	O	C	C	O	O
Col-100 B & Col-100 A	O	C	O	O	C	O	C	O	O	C	O
Only Col-100 A	O	O	C	C	C	C	C	C	O	C	O
Only Col-100 B	O	C	O	C	C	C	C	C	C	O	O

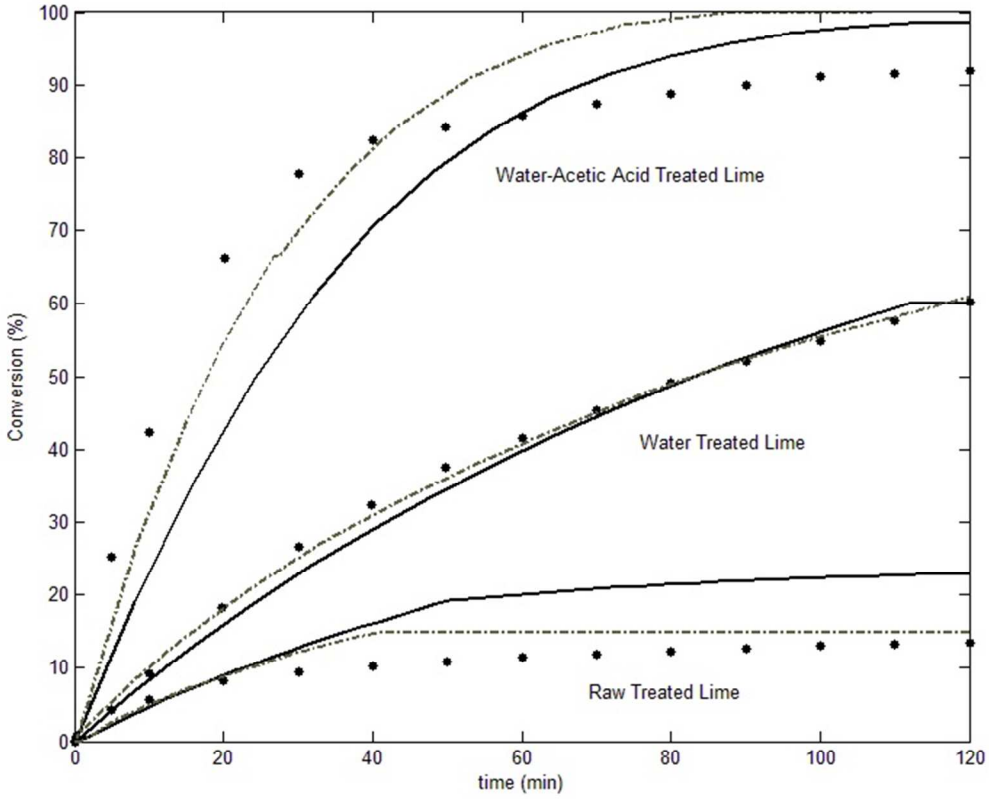

Figure 1

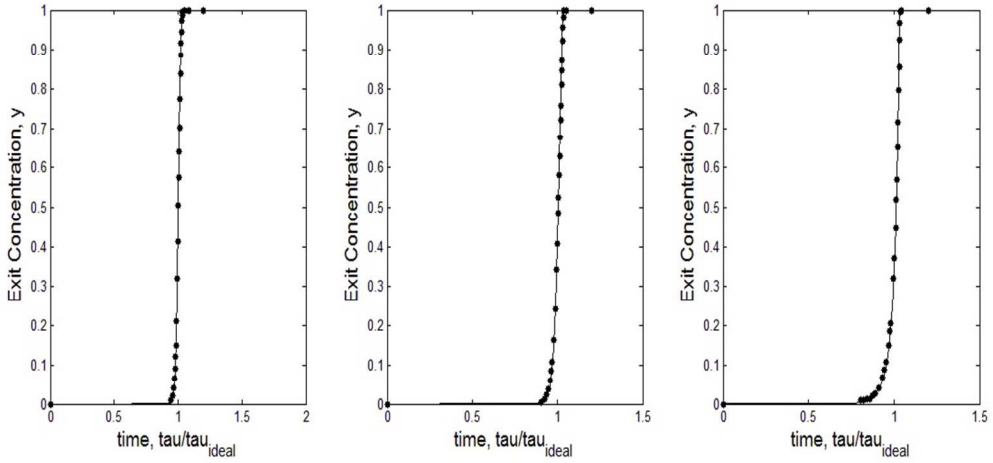

Figure 2

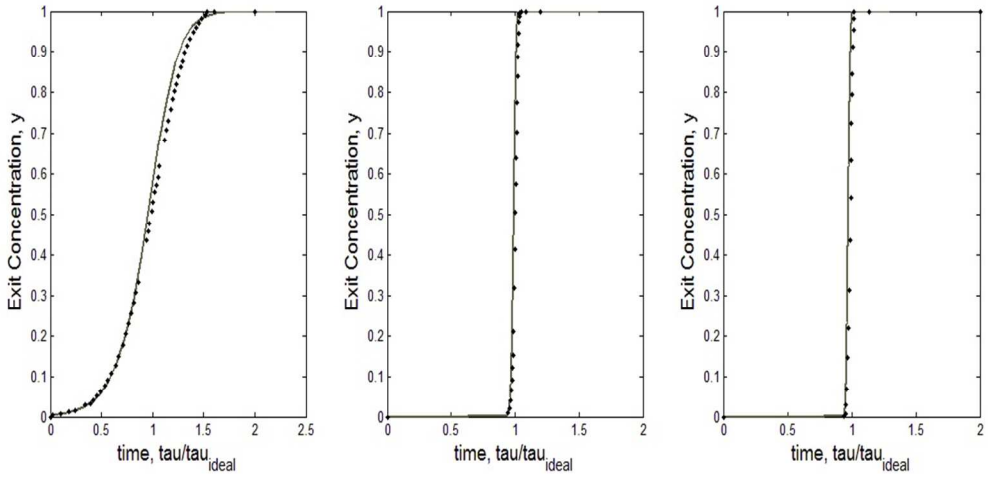

Figure 3

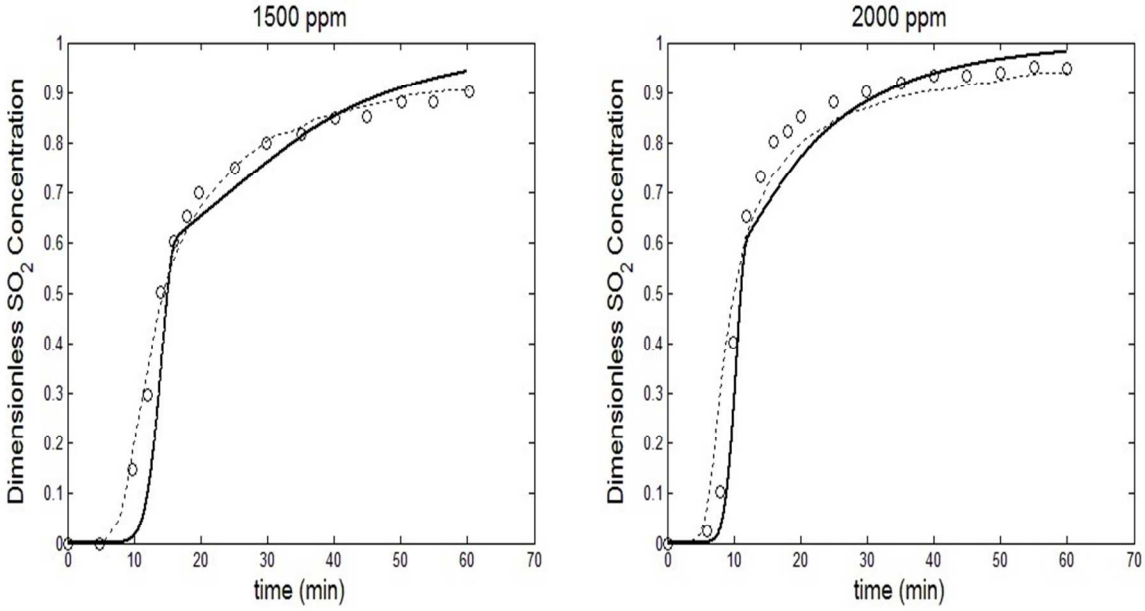

Figure 4

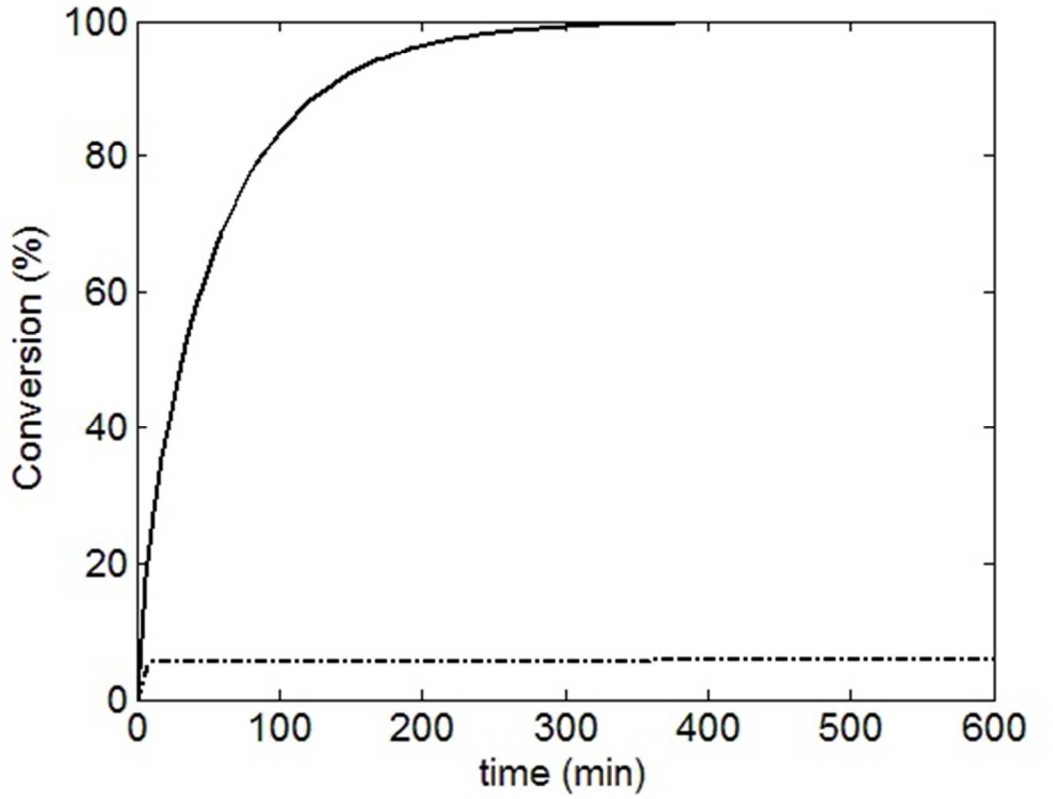

Figure 5

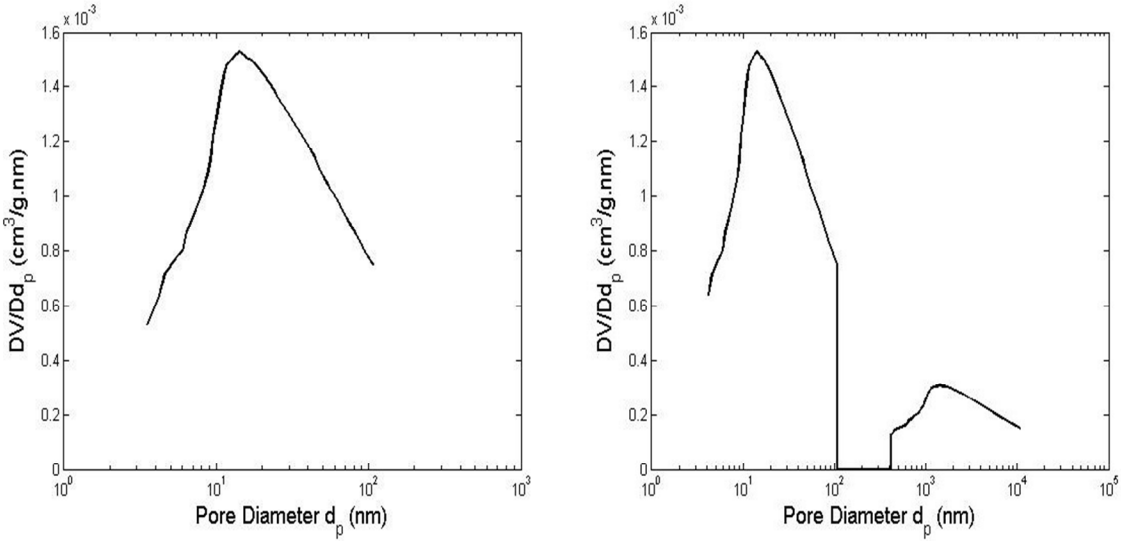

Figure 6

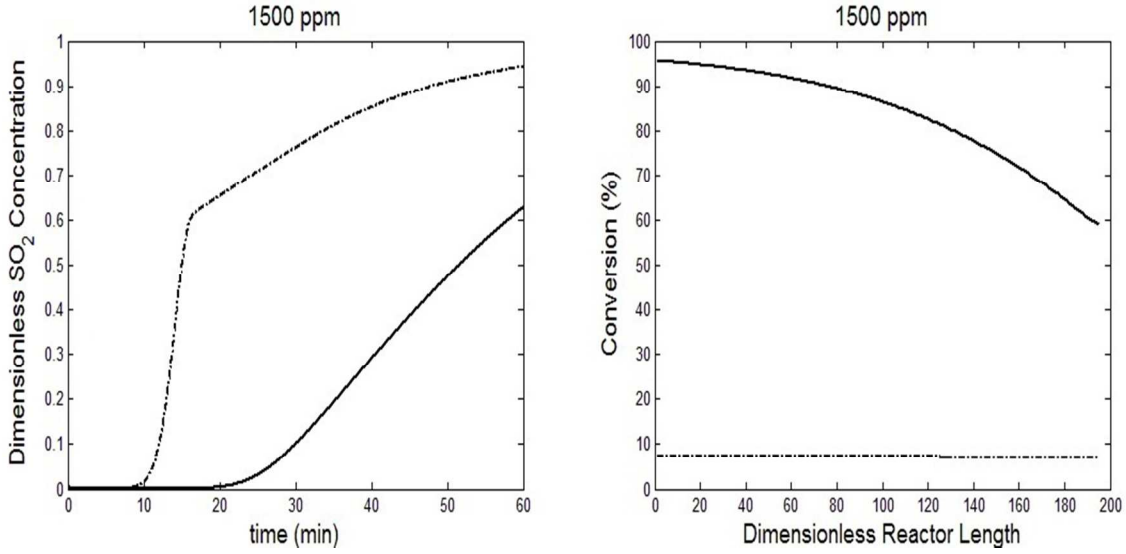

Figure 7

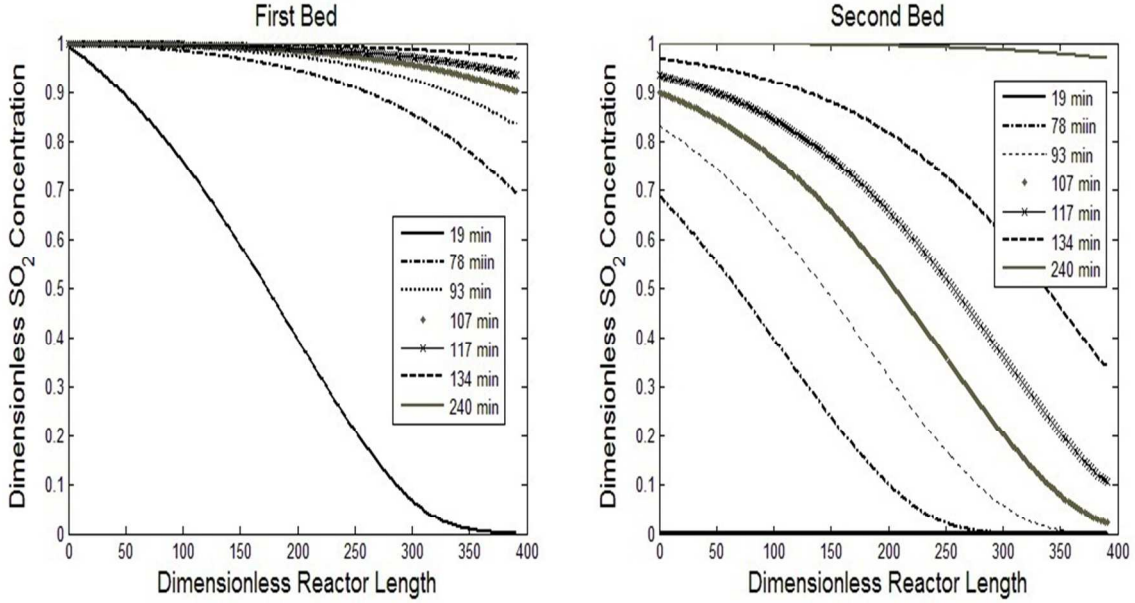

Figure 8

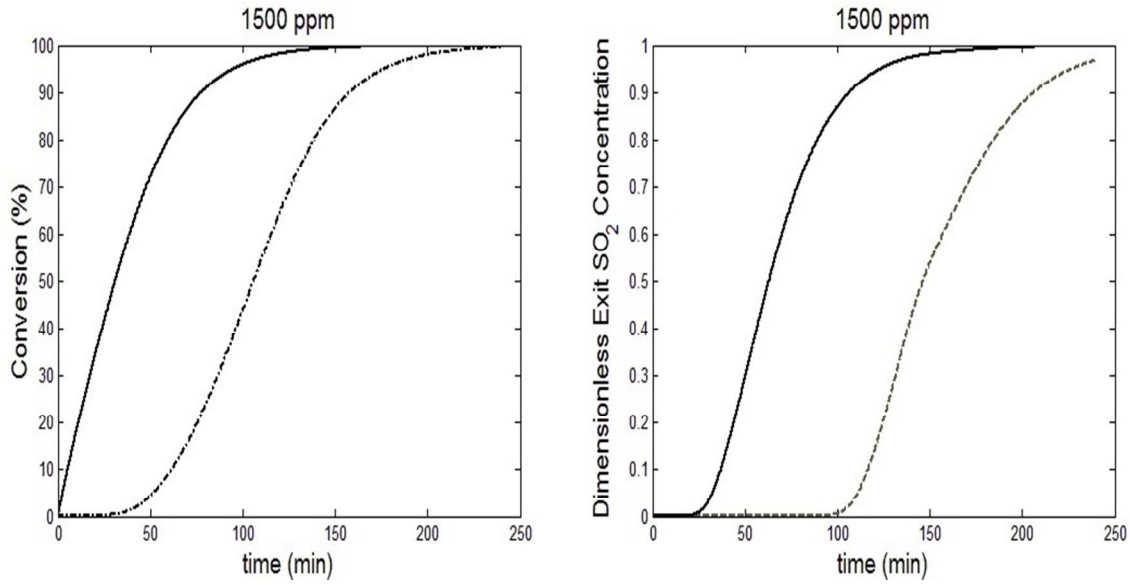

Figure 9

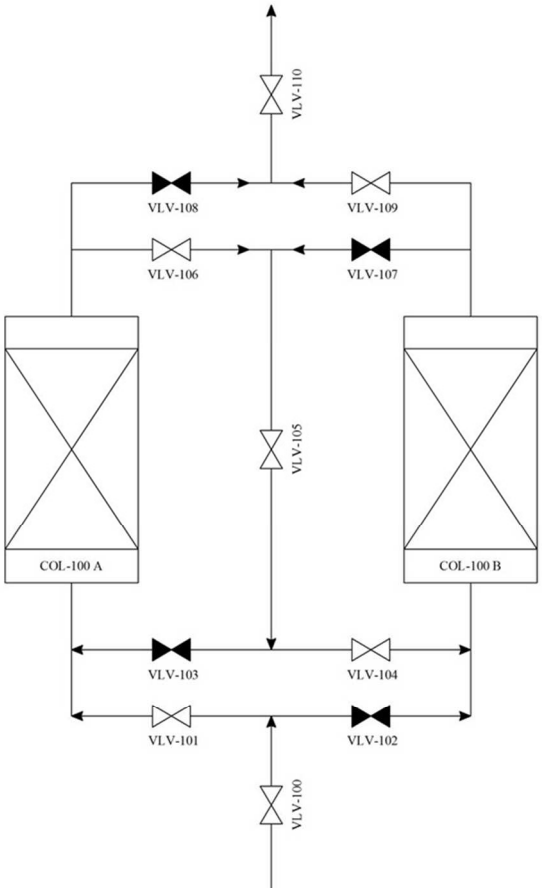

Figure 10

Random pore model differential equations in packed bed reactor for SO_2 removal by lime were solved with finite element method

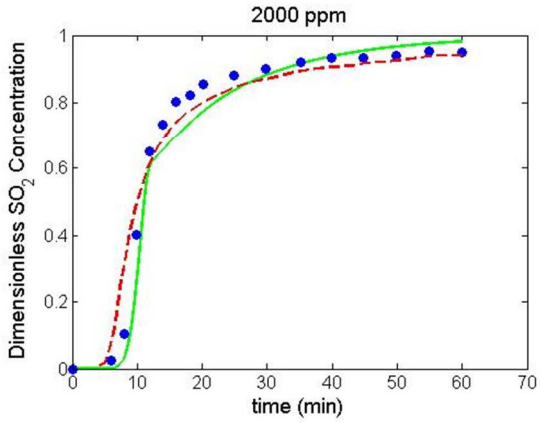

Desulfurization breakthrough curve for FE solution of random pore model (green), FD solution of shrinking unreacted core model (red), and literature experimental data (blue points)